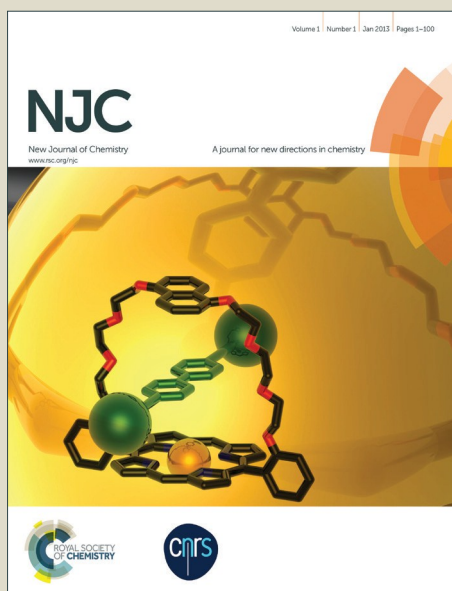


NJC

Accepted Manuscript



This article can be cited before page numbers have been issued, to do this please use: C. Li, W. yang, W. zhou, M. zhang, R. xue, M. li and Z. cheng, *New J. Chem.*, 2016, DOI: 10.1039/C6NJ01558A.



This is an *Accepted Manuscript*, which has been through the Royal Society of Chemistry peer review process and has been accepted for publication.

Accepted Manuscripts are published online shortly after acceptance, before technical editing, formatting and proof reading. Using this free service, authors can make their results available to the community, in citable form, before we publish the edited article. We will replace this *Accepted Manuscript* with the edited and formatted *Advance Article* as soon as it is available.

You can find more information about *Accepted Manuscripts* in the [Information for Authors](#).

Please note that technical editing may introduce minor changes to the text and/or graphics, which may alter content. The journal's standard [Terms & Conditions](#) and the [Ethical guidelines](#) still apply. In no event shall the Royal Society of Chemistry be held responsible for any errors or omissions in this *Accepted Manuscript* or any consequences arising from the use of any information it contains.

Branching effect for aggregation-induced emission in fluorophores containing imine and triphenylamine structure

Chunchun. Li^a, Wen Yang^a, Weiqun. Zhou^{a*}, Mengmeng. Zhang^a, Renyu. Xue^b, Mengying. Li^b, Zhongqin. Cheng^b

Received 00th January 20xx,
Accepted 00th January 20xx

DOI: 10.1039/x0xx00000x

www.rsc.org/

Three new chromophores incorporating donor- π -donor- π -donor structural motifs and single, double and triple branched 4-(N, N'-dimethylamine) phenyl groups linked to triphenylamine through an imine π -bridge were synthesized. The photoluminescence properties of three chromophores were studied in solution and aggregated states. It was demonstrated that aggregation-induced emission (AIE) effect enhanced with the increase of the branch number. The mechanism of AIE for three compounds was explained by molecule stacking mode in crystal structures. The propeller shaped non-planar molecular configuration of tri-branched triphenylamine inhibited face to face π - π stacking, which provided favorable 3D structures to restrict intramolecular rotation and benefited AIE effects. TEM, DLS and fluorescent microscope imaging revealed the nano-size of aggregate state in THF-H₂O mixture solution. Fluorescence imaging experiments of tri-branched chromophore in living A549 cells proved its possibilities for the real-world applications.

1 Introduction:

Usually, the structural design strategy of organic fluorophores has been used to enlarge the extent of π -conjugation by melding more and more aromatic rings together. The bigger discotic plates can produce high fluorescence in the dilute solutions, but fluorescence usually can be quenched in concentrated solutions and solid state, which is named ACQ (aggregation-caused fluorescence quenching) because of π - π stacking and other non-radiative pathways^[1-3], such as forming excimers and exciplexes. The ACQ effect is generally restricted for the real-world applications.^[4-8] For example, as conventional organic materials are insoluble in water, the materials of the ACQ effect cannot be used as sensors to detect biological molecules in physiological buffers and as probes to monitor ionic species in river water^[9,10]. The ACQ effect is also a thorny obstacle to the fabrication of efficient organic light-emitting diodes (OLEDs)^[11], because the luminescent materials used as emitter layers in the light-emitting devices must be fabricated in a solid film form.

The appearance of aggregation-induced emission (AIE) and/or aggregation-induced enhanced emission (AIEE) effect of fluorophore in the solution aggregated or in the solid state have opened up a new way to fluorescence materials application^[12, 34]. The AIE or AIEE effect has been attributed to the restricted intramolecular rotation (RIR) by intermolecular

steric interactions in the aggregate state. It has been realized that rational RIR in the aggregate state of AIE-active fluorophores closes the possible non-radiative decay channels and activated radiative decay channels and leads to the strong fluorescence. The covalent bonds have also been used to fasten the aryl rotors to internally set off the RIR process at the molecular level.^[13-16] Some typical examples of the AIE systems have been developed such as hexaphenylsilole (HPS)^[17,18], which has a propeller shaped non-planar molecule.

Usually, the nonplanar triphenylamine (TPA) moiety has been employed as an activator for aggregation-induced emission in the construction of AIE-active luminogens associated with its propeller-like structure and excellent electron-donating character. The present contribution finds a distinctive approach for multi-branched triphenylamine. Indeed, the multi-branched strategy constitutes a relevant tool to modulate aggregated state of AIE-active fluorophores without drastic impacts on the energy position of the electronic transitions^[19-23]. In this article, we showed that our systems appeared as aggregation induced fluorescence generators. The multi-branched construction was covalently linked to triphenylamine centers to induce hindered rotation and the desired emission enhancement. The fluorescence enhancement increased in aggregated states with the increase of multi-branched and the steric hindrance. Meanwhile, the emission wavelength was red shift gradually.

^aSchool of Chemistry & Chemical Engineering and Material Science, Soochow University, 199 Ren'ai Road, Suzhou, People's Republic of China, 215123

^bSchool of Biology and Basic Medical Sciences, Soochow University, 199 Ren'ai Road, Suzhou, People's Republic of China, 215123

2 Experimental section

2.1 Materials and instruments

Triphenylamine, N, N-dimethyl-p-phenylenediamine, POCl₃, DMF, NaOH, CH₂Cl₂, THF, MgSO₄, CH₃COOH, DMSO, acetone, CDCl₃ and MTT were used as HPLC grade purchased from J&K (CHINA). IR spectra were obtained in KBr discs using a Nicolet 170SX FT-IR spectrometer. Elemental analyses were performed on a Yanco CHNSO Corder MT-3 analyzer. ¹H NMR has been recorded on INOVA 400 at 400.13MHz, with TMS as internal standard using CDCl₃ as deuterated solvents with chemical shifts reported as ppm. Mass spectra were recorded on a Finnigan MAT95 mass spectrometer (ESI⁺). The absorption and fluorescence spectra were recorded on a CARY50 UV-VIS spectrophotometer and an FLS920 fluorescence spectrophotometer. Fluorescence quantum yields (Φ_f) in pure THF and THF/water mixtures determined with anthracene as the fluorescence reference in ethanol ($\Phi = 0.27$). The transmission electron microscope (TEM) images of the aggregations were obtained by Tecnai G220. The fluorescence microscope imaging of the nano-aggregations was obtained by Leica DM2500M. The cell images were gathered with the inverted fluorescence microscope (Olympus, IX71) and processed with Nikon AY software. All the experiments were carried out at room temperature.

2.2. Single crystal X-ray diffraction

The single crystals of compounds were obtained by the slow diffusion of their respective CH₂Cl₂/cyclohexane solutions for several days at room temperature. Since the two crystals were stable under ambient condition, the data collection was done without any inert gas protection at room temperature on a Bruker SMART APEX-II CCD area detector using graphite-monochromated Mo K α radiation ($\lambda = 0.71073 \text{ \AA}$). Data reduction and integration, together with global unit cell refinements were done by the INTEGRATE program of the APEX2 software. Semi-empirical absorption corrections were applied by using the SCALE program for area detector. The structures were solved by direct methods and refined by the full matrix least-squares methods on F2 using SHELX.

2.3 Cell culture and fluorescence imaging

Adenocarcinoma lung cells (A549) were purchased from the Shanghai Institute of Cell Biology. The cells were cultured in Roswell Park Memorial Institute culture medium (RPMI-1640), supplemented with 6% calf serum, penicillin (100 U·mL⁻¹), streptomycin (100×10⁻⁶ g·mL⁻¹) and 2.5×10⁻⁴ mol·L⁻¹ glutamine at 37°C in a 5% CO₂ incubator. The cells were cultured in a 15 mm diameter cell culture dish for 2 days. A549 cells were incubated with the tri-branch dye at a final concentration of 50 $\mu\text{g}\cdot\text{mL}^{-1}$ for 30 minutes, and washed with PBS buffer to remove extracellular material. Then the dish was placed under an inverted fluorescence microscope (Olympus, Cell'R) equipped with an objective lens (Olympus, IX71) to get long-term images at 450 nm ($\lambda = 380 \text{ nm}$).

2.4 Computational methods

The geometries for the compounds were optimized by density functional theory (DFT) calculations using the Becke-3-Lee-Yang-Parr (B3LYP) at the level of 6-31G (d) with Gaussian

09 program^[24, 25]. The vibrational frequency analysis was carried out to ensure that the obtained geometries represent minima on the potential energy surface.

3. Result and Discussion

3.1 Synthesis

The synthetic route was shown in Scheme 1.

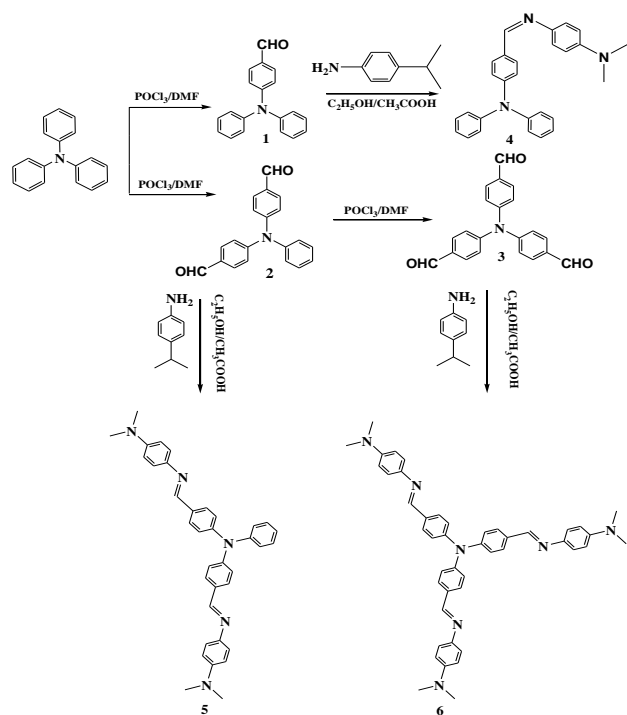
4- (diphenylamino) benzaldehyde (compound 1): 30ml dry DMF was ice-bathed and 29.5mL POCl₃ was added dropwise. After they were stirred for 40 minutes under 0°C, the temperature was raised to room temperature. Then 2.5g triphenylamine was added and the reaction mixture was heated at 45°C and stirred for 14 h. After cooling down to room temperature, the reaction mixture was poured into ice-bath and neutralized with NaOH, then extracted with chloroform. The combined organic layer was dried with magnesium sulfate anhydrous, filtered. With the organic layer concentrated, the white purified compound was obtained by using a column chromatograph of silica gel with ethyl acetate-petroleum ether mixture (1:10 v/v) as the eluent. Yield: 2.5g (90%). ¹H-NMR (DMSO, 400MHz) δ (ppm): 9.76(s, 1H), 7.71(d, 2H), 7.41(t, 4H), 7.21(m, 6H), 6.88(d, 2H).

Bis (4-benzoyl) aniline (compound 2)、Tris (4-benzoyl-yl) amine (compound 3): The compound 2 and 3 were prepared according to the general procedure for compound 1 by using 15.5 mL dry DMF, and 19 mL POCl₃, and 2.0 g triphenylamine or 5.8 mL dry DMF, and 7.6 mL POCl₃, and 0.98g bis (4-benzoyl-yl) aniline. Compound 2: Yield: 2.2g (90%). ¹H-NMR (DMSO, 400 MHz) δ (ppm): 9.87(s, 2H), 7.84(d, 4H), 7.47(t, 2 H), 7.31(s, 1 H), 7.21(d, 2H), 7.16(d, 4H). Compound 3: Yield: 0.86g (90%). ¹H-NMR (DMSO, 400MHz) δ (ppm): 9.94(s, 3H), 7.91(s, 6H), 7.28(s, 6H)^[26, 27].

Compound 4 : 20mmol 4- diphenyl--amino benzaldehyde and 20 mmol N, N- dimethyl-p-phenylenediamine were added to flask, then 10 mL ethanol and 1 to 2 drops of glacial acetic acid. The reaction mixture was then heated at 50°C and stirred for 7 h. After cooling down to room temperature and filtered, the green powder was obtained, and recrystallized from ethanol as yellow solid. Yield: 0.55g (70%). Anal. calc. formula: C₂₇H₂₅N₃. (%): C: 82.86; H: 6.39; N: 10.74; Found: C₂₇H₂₅N₃. (%): C: 82.30; H: 6.40; N: 10.83. IR: 1609cm⁻¹ (ν C=N), 1168cm⁻¹, 1290cm⁻¹, 1325cm⁻¹ (ν C-N), 2794cm⁻¹, 2840cm⁻¹ (ν C-H, -CH₃). ¹H-NMR (400 MHz, DMSO) δ (ppm): 8.37(s, 1H), 7.30(t, J=10, 8H), 7.16(d, J=10.81, 6H), 7.07(d, J=11.6, 6H), 6.76(d, J=11.6, 2H), 2.98(s, 6H). HRMS calc. for (M + H⁺)⁺: 391.2048, found: 392.2144

Compound 5 and compound 6: The compound 5 and compound 6 were prepared according to the general procedure for compound 4 by changing the ratio of bis(4-benzoyl)aniline and N, N- dimethyl-p-phenylenediamine. Compound 5: Yield: 0.7g (65%). Anal. calc. formula: C₃₆H₃₅N₅. (%): C: 79.65; H: 6.57; N: 12.89; Found: C₃₆H₃₅N₅. (%): C: 80.44; H: 6.51; N: 13.04. IR: 1620cm⁻¹ (ν C=N), 1169cm⁻¹, 1286cm⁻¹, 1310cm⁻¹ (ν C-N), 2802cm⁻¹, 2853cm⁻¹ (ν C-H, -CH₃). ¹H-NMR (400 MHz, DMSO): δ (ppm): 2.92(s, 12H), 6.76(d, J=7.5,

4H), 7.24(m, 11H), 7.40(t, J=8.0, 2H), 7.80(d, J=4.4, 4H), 8.56(s, 2H). HRMS calc. for (M + H)⁺: 537.2892, found: 538.2968. Compound 6: Yield: 0.76g (55%). Anal. calc. formula: C₄₅H₄₅N₇. (%): C: 78.94; H: 6.43; N: 13.96; Found: C₄₅H₄₅N₇. (%): C: 79.06; H: 6.59; N: 14.35. IR: 1618cm⁻¹(νC=N), 1167cm⁻¹, 1281cm⁻¹, 1316cm⁻¹ (νC-N), 2797cm⁻¹, 2848cm⁻¹ (νC-H, -CH₃); ¹H-NMR (400 MHz, DMSO) δ (ppm): 2.92(s, 18H), 6.75(d, J=8.4, 6H), 7.17(d, J=8.4, 6H), 7.25(d, J=8.4, 6H), 7.85(d, J=8.4, 6H), 8.6(s, 3H). HRMS calc. for (M + H)⁺: 683.3736, found: 684.3172.



Scheme 1 the synthetic route of branched compounds

3.2. Photo-physical and AIE Properties

The absorption spectra of the three compounds in THF were shown in Fig. 1(a). From Fig.1, the low energy side of the spectra was dominated by a broad and structure less band at greater than or equal to 380 nm and underwent a bathochromic shift from 4, 5 and 6. The bathochromic shift of the transition band of all compounds could be attributed to the enhanced electronic coupling between the 4-(N,N'-dimethylamino)phenylimine and triphenylamine, which resulted in the more extended π-conjugation length on the long axis of the molecule.^[28, 29] Single branch chromophores (4) exhibited a second distinctive band near 300 nm, which should be ascribed to electronic transitions centred on the triphenylamine moiety. The absorption peak appeared in the manner of shoulder for both double and triple chromophores (5 and 6). The fluorescent emissions were displayed under a 380 nm UV lamp and the fluorescence quantum yield was lower than 1% (Table1). Stokes shift (Δλ) was between 83 and 95 nm, which was analyzed by the intramolecular charge transition (ICT). The band red shift clearly levelled off when considering the multi-branched compounds for both UV and PL spectra. Fig. 1(b) showed the normalized absorption and fluorescence spectra of double-branched compound (5) in various solvents. Contrary to the absorption spectra, the fluorescence bands underwent a pronounced bathochromic shift with the increase of solvent polarity. This solvent induced effect provided a clear evidence for TICT (twisted intramolecular charge transfer) process^[30-32] of the fluorescence singlet states.

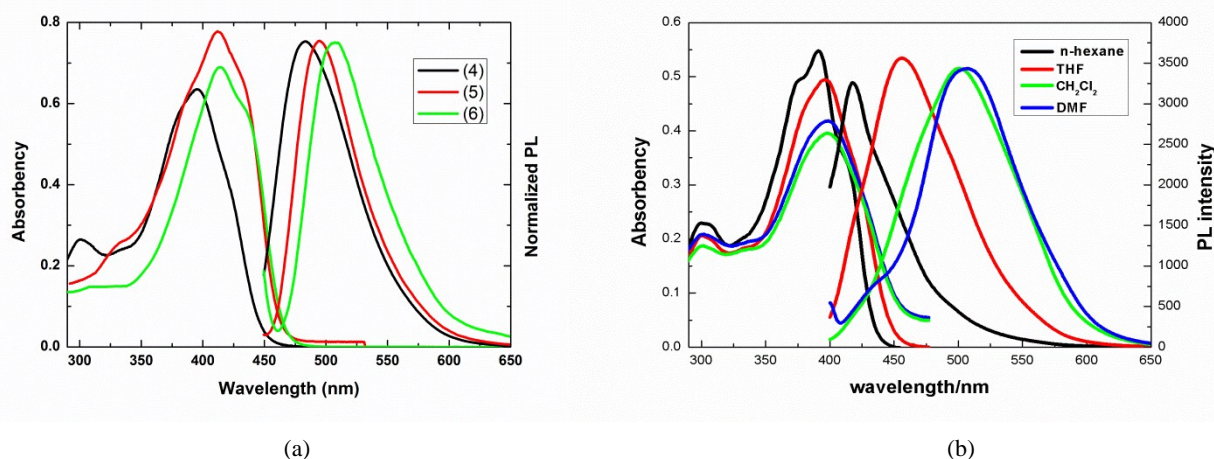


Fig. 1 (a) UV- spectra and fluorescent emissions of single- (4) double- (5) and triple-branched (6) triphenylamine derivatives in THF solution (1×10^{-5} M); (b) absorption and normalised emission spectra of double branch compound (5) in various solvents

A solvent-poor-solvent photoluminescence (PL) test, which was commonly used for studying the AIE phenomenon,^[33-35] was performed to investigate the luminescent behavior of the purpose compounds. The molecules would aggregate in

THF/water mixtures with high water contents because of its insolubility in water, and the luminescence of such systems was primarily attributed to molecule aggregation. The dispersion system of nano-aggregated was obtained by the

gradual addition of water into THF with different ratios.^[36] AIE effect (I/I_0)^[37] of three derivatives was drawn in Fig.2 (a-c). The formation of aggregates can also be confirmed by the changes of UV-vis, PL spectra and fluorescence microscope imaging in THF/water mixtures with various water volume fractions (f_w). Single-branched chromophore (compound 4) (Fig.2(a)) exhibited the strong absorption peaks at 395 nm and the weak absorption peaks at 301 nm in pure THF solution. With an increase of f_w from 0% to 90%, the strong peaks decreased and the weak peak increased. At the same time, in the solvent mixtures, the levelled-off tails appeared in the visible region when f_w was equal to 90%, indicating that the aggregates were probably at nanoscale sizes. However, there were no levelled-off spectral tails in the long-wavelength region in UV-vis spectra with f_w equal to 80% or less than. Single-branch chromophore (compound 4) in dilute THF solution (5×10^{-5} mol/L) emitted blue fluorescence at 483 nm (QY=0.79%) (Table 1). The fluorescence intensity decreased when the f_w increased to 40%, and then increased as the content of water increased. When f_w was equal to 80%, the fluorescence of the solution increased to a maximum value, the fluorescence strength was equivalent to that in pure THF (Fig.2 (d) and Table 1). In addition, the levelled-off tails appeared in the visible region of UV spectra when f_w was equal to 80%, indicating that the aggregates were probably at nanoscale sizes. Inserted picture in Fig.2 (a) was fluorescence microscope imaging of 4 when f_w was equal to 80%, which indicated the appearance of the aggregated fluorescence.

The influence of steric hindrance effects on the AIE

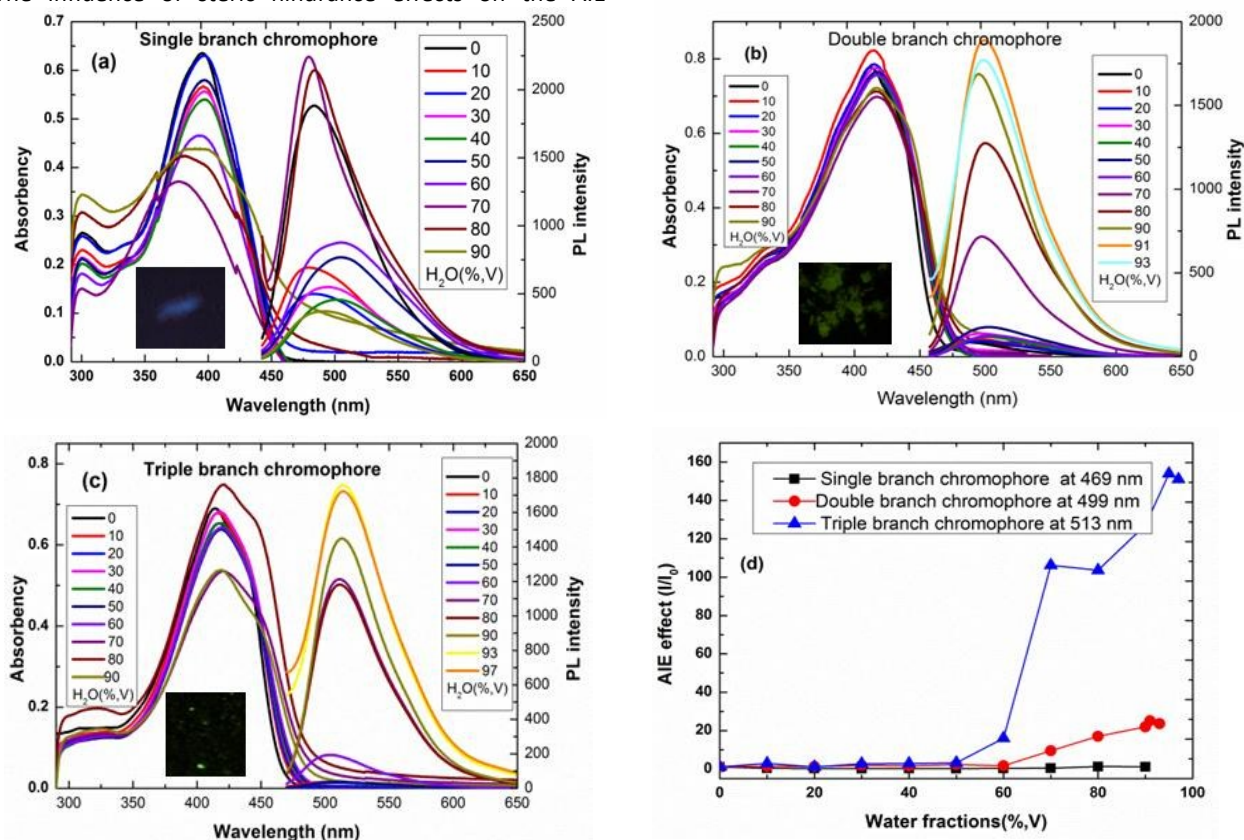


Fig. 2(a-c) The UV- spectra (left) and Emission spectra (right) of triphenylamine derivatives in THF–water mixtures (5×10^{-5} M) with different water fraction (f_w). (inset: fluorescence spectra microscopic picture of triphenylamine derivatives water under 365 nm irradiation). (d) AIE effect (I/I_0) of triphenylamine derivatives.

properties was investigated by introduction of multi-branched donor substituted into triphenylamine central. The outstanding fluorescence enhancement in aggregation state was exhibited with increasing the branch numbers of the donor. As shown in the Fig.2 (b), when the water fraction increased to 91%, double-branched triphenylamine (compound 5) exhibited emission enhancements of 25.1- fold (Fig.2 (b) and Table 1) in THF/water mixture solutions, compared to that in pure THF (Fig.2(c)), and the fluorescence quantum yield (Φ_f) was determined to be 5.1% using anthracene as a fluorescence reference ($\Phi_f = 0.27$ in ethanol) (Table 1)^[38]. When f_w was equal to 91%, the fluorescence microscope imaging of 5 in aggregated state was shown in the inserted picture of Fig.2 (b). AIE effect enhancement of 5 should be due to their more twisted conformations caused by the increase of the substituent group on the phenyl ring. Fig.2(c) showed the AIE effect of tri-branched triphenylamine (compound 6). When f_w was equal to 93%, 6 exhibited the fluorescence enhancements of 157- fold (Fig.2(d) and Table 1) compared to that in THF (Fig.2(c)), and the Φ_f were determined to be 16.2% (Table 1)^[39, 40]. Fluorescence microscope imaging showing bright green fluorescence of 6 was inserted in Fig.2 (c) ($f_w = 93\%$). The strongest AIE effect of 6 in all three compounds confirmed further that steric hindrance was advantageous to the enhancement of the AIE effect.^[41]

Table 1 The maximum absorption (λ_a , nm), DFT calculation results (nm), the maximum emission wavelength, (λ_{em} , nm), fluorescence quantum yield (Φ_f , %) and AIE effect (I/I_0) of three compounds in THF and THF/H₂O View Article Online
DOI: 10.1039/C6NJ01558A

	THF				THF-H ₂ O			
	$\lambda_{a,max}$ (nm)	DFT	λ_{em} (nm)	Φ_f (%)	λ_{em} (nm)	H ₂ O%	Φ_f (%)	I/I_0^a
1	395	409	483	0.79	480	80	0.81	1.2
2	412	446	495	0.21	503	91	5.1	25.1
3	413	454	508	0.11	514	95	16.2	157

^a I/I_0 : the proportion of Φ_f in THF to Φ_f in THF–water.

3.3 Theoretical studies

To better understand the spectral behavior, the fully optimized structures of three compounds were carried out at the level of B3LYP/6-31G (d). Molecular orbital amplitude plots of the highest occupied molecular orbital (HOMO) and the lowest unoccupied molecular orbital (LUMO) of three derivatives were depicted in Fig.3. All three dyes showed quite similar structures since the triphenyl moiety globally present a D₃-like symmetry with twisted angles around the bond connecting the central nitrogen atom to the phenylene rings.^[42, 43] Time-dependent (TD) combining with a SCRF method (CPCM, by THF as solvent) at the same level were applied to indicate the

energies of HOMO and LUMO. Table1 showed the energy gaps of the HOMO and LUMO orbital of DFT predicted and UV absorption. In Table 1, the calculated energy gaps between the HOMO and LUMO were close to the corresponding UV absorption energies. The energy gap (HOMO to LUMO) were 3.03 eV (409nm), 2.78 (446 nm) and 2.73(454 nm) for single-branched (4), double-branched (5) and triple-branched compound (6) respectively. The energy gap decreased with branch number enhancement, which corresponding to the bathochromic shift in the UV spectra with branch number enhancement. As shown in Fig. 3, the longest wavelength electronic transition indicated an electronic delocalization all along the compound structure (π - π^* type) with a very slight charge transfer from the amino group to the phenylimine moieties.

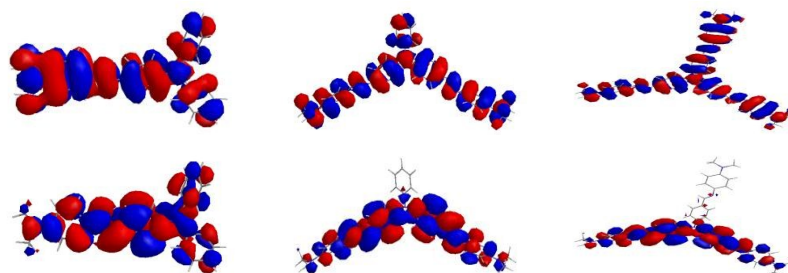


Fig. 3 HOMO(bottom) and LUMO(top) orbital from left to right, single, double and triple branch compounds computed by the B3LYP/6-31G(d) level of the theory.

3.4 Crystal structures and mechanisms of AIE

In order to better understand the relationship between the photophysical properties and the molecular packing, the single crystal of three triphenylamine derivatives were prepared through slow evaporation of acetonitrile solution at room temperature.^[44, 45] X-ray molecular structures and crystallographic packing of three chromophores were depicted in Fig.4-6. As shown in Fig.4-6, all three compounds showed quite similar structures since the 4-(N,N'-imethylamine)phenylimine branches adopted a quasi-planar conformation, the angles between the benzylidene and 4-N,N'-dimethylphenylimido were 56.29° (single branched), 9.2° (double branched) and 21.3°, 33.0° and 35.0°(triple branched), which indicated the conjugation between the benzylidene and 4-N,N'-dimethylphenylimido with the increased of branches. It led to the gradually bathochromis-shifts from single-, double- and tri-branched triphenylamine of both absorption and emission bands. The maximum absorption wavelength was

395, 412 and 413 nm and the maximum emission wavelength was 483, 495 and 508 nm for single-, double- and tri-branched triphenylamine in THF respectively. X-ray molecular structure and crystallographic packing of single branch compound (4, CCDC number: 1495312) were depicted in Fig.4 (a) and Fig.4 (b). The triphenyl moiety globally present a D₃-like symmetry with twisted angles around the bond connecting the central nitrogen atom to the phenylene rings, which agreed with the result of DFT calculations. The angle between two phenyl rings was 82.6°, and the angles between two phenyl ring and 4-N,N'-dimethylphenylimido were 62.6° and 64.1° respectively. In crystallographic packing (Fig. 4(b)), on the one side, adjacent molecules were stacked by C22–H22/C11 weak interactions ($d = 2.875\text{\AA}$), which led to the weak π - π stacking interaction and the distance between two planes (C6C7C8C9C10C11) of the adjacent molecules was 3.333 Å. The face-to-face stacking caused the quenched emission in the crystalline aggregated state. On the other side, another weak interactions C4–H4/N2

(2.643 Å) between adjacent molecules compelled a J stacked model and the J-type aggregate equally resulted in the increase of the fluorescence intensity in the crystalline

aggregated state. So, the fluorescence strength in aggregated state was equivalent to that in pure THF. DOI: 10.1039/C6NJ01558A

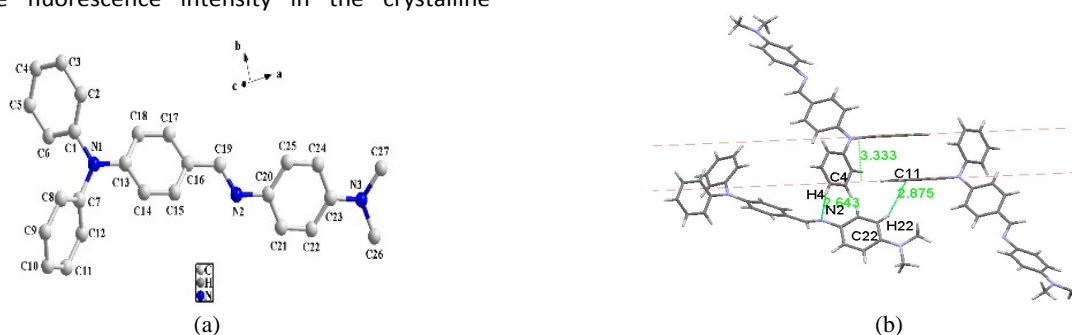


Fig. 4 X-ray molecular structure (a) and crystallographic packing (b) of single branch compound (4)

The molecule of 5 (CCDC number: 1495311) had a C_{2v} symmetry (Fig. 5(a)). The angles between phenyl ring and two 4-N, N'-dimethylphenylimido were 63.2° and the angles between two 4-N, N'-dimethylphenylimido were 80.7° . The symmetry structures were beneficial to co-plane between two imine branches of adjacent molecules, which were the main driving force for the formation of symmetric dimers, which also locked the intramolecular rotations of the phenyls (Fig. 5(b)). The adjacent molecules were stacked through C22–

H22/C11 weak interactions ($d = 2.867 \text{ \AA}$). The aggregation of 5 did not involve $\pi-\pi$ interactions. Every two molecules in 5 form a dimer and pack in a parallel but staggered style, which inhibited the $\pi-\pi$ interactions in crystal structure.^[46, 47] Thus, the stacking manner not only avoided the maximum face-to-face $\pi-\pi$ stacking that caused the quenched emission, but also decreased the vibration of molecular framework, which make for the increase of AIE effect.^[48]

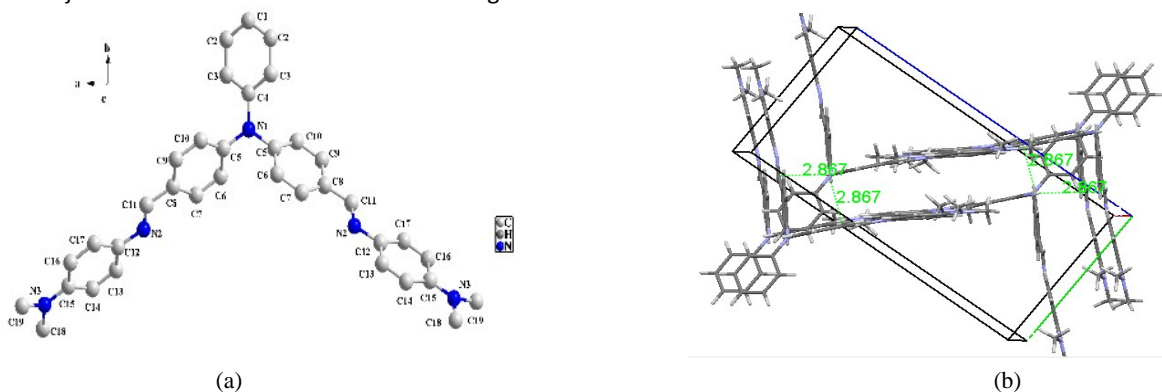


Fig. 5 X-ray molecular structure (a), crystallographic packing (b) of double branch compound (5)

Fig. 6 depicted crystal structure and crystallographic packing of the 6. In Fig. 6 (a), 6 present a propeller shaped non-planar asymmetry molecular structure due to the propeller-shaped triphenylamine unit. The angles between three 4-N, N'-dimethylphenylimido were 62.1° , 78.8° and 76.2° . In the crystal of 6 (Fig. 6 (b)), the dimers between two imine branches of adjacent molecules in double branch molecule could not be found. On the other hand, the torsion angle between 4-N, N'-

dimethylphenylimido exhibiting more twisting structure of 6 than that in 5. And, one branch, 4-N, N'-dimethylphenylimido chain of one molecular inserted between two 4-N, N'-dimethylphenylimido chain in another molecule reduce the conjugation of molecules and prevent face-to-face $\pi-\pi$ stacking in aggregations.^[32, 49] Therefore, the vibration of molecular framework was also decreased and AIE increased.

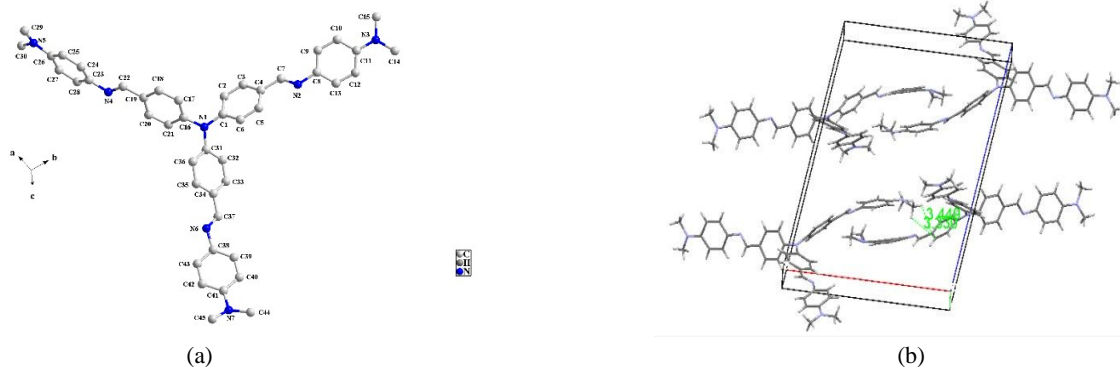


Fig. 6 X-ray molecular structure (a), crystallographic packing (b) of triple branch compound (6)

3.5 Nanoparticles fabrication and cell imaging

In order to further gain insight into the AIE mechanism of the three compounds, the size and growth process of particles with different water fractions were studied using TEM and DLS. Fig.7 showed the TEM images of triphenylamine chromophores. As shown in Fig. 7, all nanoparticles were in spherical shape with an average size of around 150 nm, 350 nm and 200 nm respectively for single-, double- and triple-branched chromophores. As can be seen from the data in table 2, it was at close proximity with TEM results while the water content increased to 80%-90%. And this result gives direct evidence of molecular aggregation during emission

enhancement. The molecules of compounds can slowly assemble in an ordered fashion to form microcrystalline but less-emissive particles in the THF-water mixtures with low water contents, while in mixtures containing very large amounts of water, the molecules of compounds abruptly agglomerate to form less-crystalline or even amorphous but more-emissive clusters, which effectively avoid π - π stacking.^[50-52]

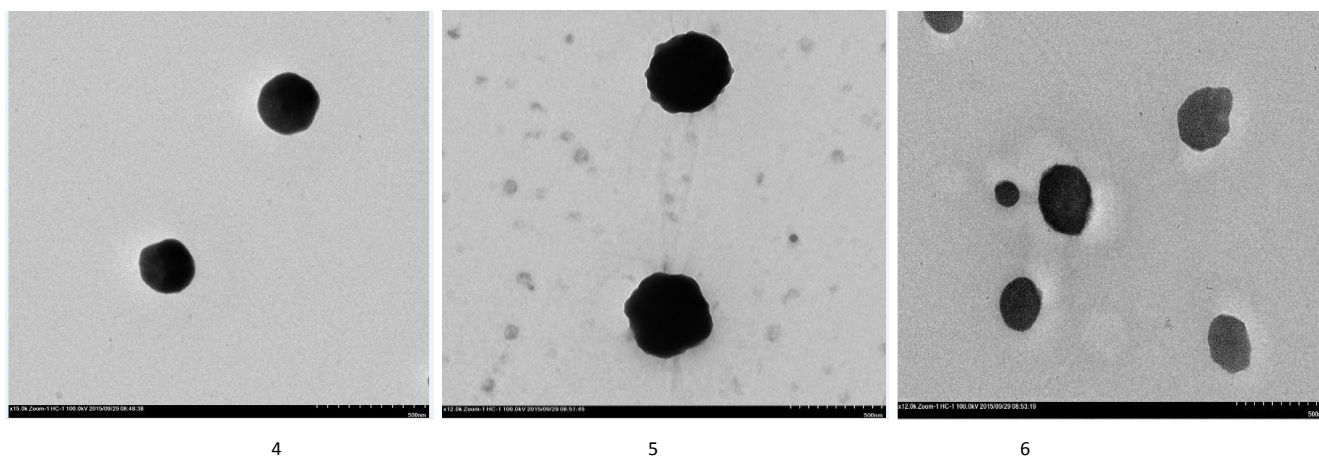


Fig. 7 TEM images of compound 4, 5 and 6 in THF-water mixtures at concentrations of 5×10^{-5} M with different water fractions (4 in THF-water (2/8, v/v); 5, 6 in THF-water (1/9, v/v)).

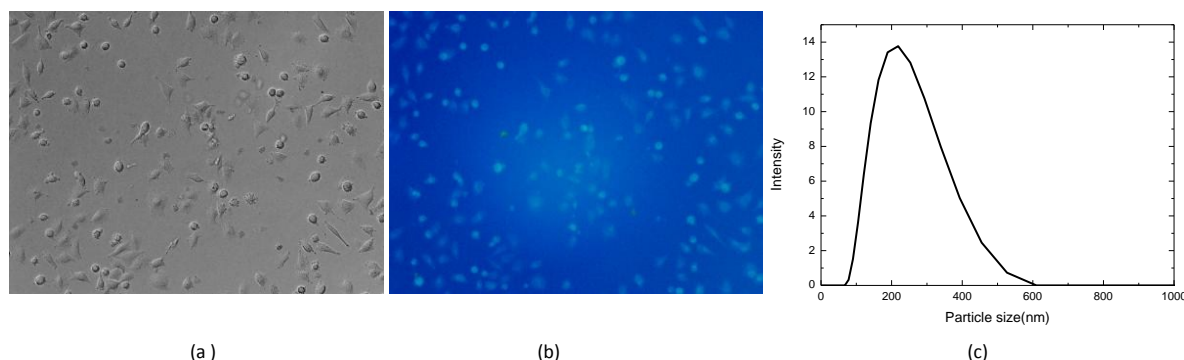


Fig.8 Fluorescence images of A549 treated with $50 \mu\text{g}\cdot\text{mL}^{-1}$ triple branch compound (6) under visible light (a) and UV irradiation (b) and DLS data for tri-branched chromophore in the cell culture fluid(c).

Table 2 The average diameter of aggregates with different water fractions (f_w) of compound 4-6

	4	5	6
$d_{f_w=40\%}$ (nm)	105	160	143
$d_{f_w=60\%}$ (nm)	140	210	146
$d_{f_w=80\%}$ (nm)	152	320	174
$d_{f_w=90\%}$ (nm)	110	357	199

View Article Online
DOI: 10.1039/C6NJ01558A

We furthered to study the potential applications of three triphenylamine chromophores in bio-imaging. Compound 6 was selected to investigate the applicability in fixed cell imaging for 6 having the highest fluorescence quantum among the three dyes. Living cell imaging of A549 was obtained at 450 nm ($\lambda=380$ nm) by inverted fluorescence microscope. The cells displayed a bright green fluorescence image. The fluorescence images were depicted in Fig.8(a) and Fig8.(b). The fluorescence and bright-field images revealed a high cell membrane permeability of 6.

To confirm the formation of aggregation inside the cells, small amount of 6 was added to the cell culture fluid to simulate the cell environment, and dynamic light scattering (DLS) measurement was conducted. As it was shown in Fig.8(c), the average diameter of the particle was 192.3nm, which indicated the formation of aggregation inside the cells. 6 could probably permeate the cell membrane in the solution state, and aggregate inside the cell.^[53-55]

As for intracellular imaging applications, the cytotoxicity of the probe should be taken into consideration. The MTT assay was performed to evaluate the toxicity of 6 by A549 cells. 8-16-24 h incubation was taken at the same condition. The experimental data were expressed in Table 3. Compound 6 exhibited a little cytotoxicity for cells, and at the concentration of 20 μ M, the cell viability was still more than 83%, which indicated a good biocompatibility of 6.

Table 3 Cell survival with different concentration of tri-branched chromophore after 8, 16, 24h.

Concentration ($\times 10^{-5}$ mol L ⁻¹)	Cell survival		
	8h	16h	24h
0	99%	99%	99%
0.5	95%	95%	90%
1.0	93%	90%	88%
1.5	90%	88%	88%
2.0	85%	85%	83%

4 Conclusions

Three compounds linked to triphenylamine and single, double triple branched 4-(N,N'-dimethylamine) phenyl groups through an imine π -bridge were synthesized and their structures were characterized by NMR, IR, and element analysis. The photoluminescence properties in solution and AIE effects in aggregation states of three chromophores were studied in THF-H₂O mixture solutions. The particle diameter of three

compounds in THF-H₂O mixture solutions was shown by TEM and DLS which indicated the aggregation of three chromophores. We employed the X-ray single crystal structures of three compounds and theoretical calculations to reveal the AIE mechanism. In the crystal packing, we found that the inhibited face to face π - π stacking and favorable 3D structures would restrict intramolecular rotation and make AIE effect enhance with the increase of branch number. Fluorescent microscope imaging also indicated AIE effect. Furthermore, fluorescence imaging of the 6 in living A549 cells provided evidence of its potential for practical applications in biological systems.

Acknowledgments

This work was supported by the National Natural Science Foundation of China (No. 51079094) and the Natural Science Foundation of Jiangsu Province (No. BK2010215). The Project was funded by the Priority Academic Program Development of Jiangsu Higher Education Institutions.

Notes and references

- 1 A. C. Grimsdale, K. Mullen, *Angew. Chem. Int. Ed.*, 2005, **44**, 5592.
- 2 J. L. Geng, K. I. Li, D. Ding, X. H. Zhang, W. Qin, J. Z. Liu, B. Z. Tang, B. Liu, *Small*, 2012, **8**, 3655.
- 3 Q. Zheng, T.Y. Ohulchanskyy, Y. Sahoo, P. N. Prasad, *J. Phys. Chem. C.*, 2007, **111**, 16846.
- 4 W. Li, Q. D. Li, C. H. Duan, S. G. Liu, L. Ying, F. Huang, Y. Cao, *Dyes and Pigments*, 2015, **113**, 1.
- 5 M. Pawlicki, H. A. Collins, R. G. Denning, H. L. Anderson, *Angew. Chem. Int. Ed.*, 2009, **48**, 3244.
- 6 K. Li, Y. H. Jiang, D. Ding, X. H. Zhang, Y. T. Liu, J. L. Hua, S. F. Si, B. Liu, *Chem. Commun.*, 2011, **47**, 7323.
- 7 A. Bhaskar, G. Ramakrishna, Z. Lu, R. Twieg, J. M. Hales, D. J. Hagan, E. V. Stryland and T. Goodson, *J. Am. Chem. Soc.*, 2006, **128**, 11840.
- 8 T. C. Lin, Y. J. Huang, Y. F. Chen and C. L. Hu, *Tetrahedron*, 2010, **66**, 1375.
- 9 Q. Bellier, N. S. Makarov, P. A. Bouit, S. Rigaut, K. Kamada, P. Feneyrou, G. Berginc, O. Maury, J. W. Perry, C. Andraud, *Phys. Chem. Chem. Phys.*, 2012, **14**, 15299.
- 10 T. N. Kopylova, V. A. Svetlichnyi, G. V. Mayer, A. V. Reznichenko, V. M. Podgaetskii, *Quantum. Electron.*, 2003, **33**, 967.
- 11 Y. Y. Gong, J. Liu, Y. R. Zhang, G. F. He, Y. Lu, W. B. Fan, W. Z. Yuan, J. Z. Sun, Y. M. Zhang, *J. Mater. Chem. C.*, 2014, **2**, 7552.
- 12 J. D. Luo, Z. L. Xie, J. W. Y. Lam, L. Cheng, H. Y. Chen, X. W. Zhan, Y. Q. Liu, D. B. Zhu, B. Z. Tang, *Chem. Commun.*, 2001, 1740.

- 13 M. Wang, G. Zhang, D. Zhang, D. Zhu, B. Z. Tang, *J. Mater. Chem.*, 2010, **20**, 1858.
- 14 J. P. Xu, Z. G. Song, Y. Fang, J. Mei, L. Jia, A. J. Qin, *Analyst.*, 2010, **135**, 3002.
- 15 D. Ding, K. Li, B. Liu, B. Z. Tang, *Acc. Chem. Res.*, 2013, **46**, 2441.
- 16 P. Chen, R. Lu, P. Xue, T. Xu, G. Chen, Y. Zhao, *Langmuir.*, 2009, **25**, 8395.
- 17 J. Chen, C. C. W. Law, J. W. Y. Lam, Y. Dong, D. Zhu, B. Z. Tang, *Chem. Mater.*, 2003, **15**, 1535.
- 18 B. Z. Tang, X. Zhan, G. Yu, P. P. S. Lee, Y. Liu and D. Zhu, *J. Mater. Chem.*, 2001, **11**, 2974.
- 19 C. L. Devi, Y. N. S. Makarov, V. J. Rao, K. Bhanuprakash, J. W. Perry, *Dyes and Pigm.*, 2015, **113**, 682.
- 20 Z. J. Ning, Z. Chen, Q. Zhang, Y. L. Yan, S. X. Qian, Y. Cao, H. Tian, *Adv. Funct. Mater.*, 2007, **17**, 3799.
- 21 Y. Liu, X. T. Tao, F. Z. Wang, X. N. Dang, D. C. Zou, Y. Ren, M. H. Jiang, *J. Phys. Chem. C.*, 2008, **112**, 3975.
- 22 K. Shiraiishi, T. Kashiwabara, T. Sanji, M. Tanaka, *New. J. Chem.*, 2009, **33**, 1680.
- 23 H. C. Su, O. Fadhel, C. J. Yang, T. Y. Cho, C. Fave, M. Hissler, C. C. Wu, R. Reau, *J. Am. Chem. Soc.*, 2006, **128**, 983.
- 24 M. J. Frisch, G. W. Trucks, H. B. Schlegel, G. E. Scuseria, M. A. Robb, J. R. Cheeseman, G. Scalmani, V. Barone, B. Mennucci, G. A. Petersson, H. Nakatsuji, M. Caricato, X. Li, H. P. Hratchian, A. F. Izmaylov, Y. Bloino, G. Zheng, J. L. Sonnenberg, M. Hada, M. Ehara, K. Toyota, R. Fukuda, J. Hasegawa, M. Ishida, T. Nakajima, Y. Honda, O. Kitao, H. Nakai, T. Vreven, J. A. Montgomery Jr, J. E. Peralta, F. Ogliaro, M. Bearpark, J. J. Heyd, E. Brothers, K. N. Kudin, V. N. Staroverov, R. Kobayashi, J. Normand, K. Raghavachari, A. Rendell, J. C. Burant, S. S. Iyengar, J. Tomasi, M. Cossi, N. Rega, J. M. Millam, M. Klene, J. E. Knox, J. B. Cross, V. Bakken, C. Adamo, J. Jaramillo, R. Gomperts, R. E. Stratmann, O. Yazyev, A. J. Austin, R. Cammi, C. Pomelli, J. W. Ochterski, R. L. Martin, K. Morokuma, V. G. Zakrzewski, G. A. Voth, P. Salvador, J. J. Dannenberg, S. Dapprich, A. D. Daniels, O. Farkas, J. B. Foresman, J. V. Ortiz, J. Cioslowski and D. J. Fox, *Gaussian 09 Revision A.02*, Gaussian Inc., Wallingford CT, 2009.
- 25 J. Tomasi and M. Persico, *Chem. Rev.*, 1994, **94**, 2027.
- 26 T. Mallegol, S. Gmouh, M. Blanchard-Desce, O. Mongin, *Synthesis.*, 2005, **11**, 1771.
- 27 Y. B. Sun, Y. H. Sun, Q. Y. Pan, G. Li, B. Han, D. L. Zeng, Y. F. Zhang, H. S. Cheng, *Chem. Commun.*, 2016, **52**, 3000.
- 28 B. J. Xu, J. J. He, Y. Liu, B. Xu, Q. Z. Zhu, M. Y. Xie, Z. B. Zheng, Z. G. Chi, W. J. Tian, C. J. Jin, F. L. Zhao, Y. Zhang, *J. Mater. Chem. C.*, 2014, **2**, 3416.
- 29 Z. Y. Wang, Y. Y. Gong, B. Z. Tang, *Chem. Mater.*, 2012, **24**, 1518.
- 30 L. Kong, Y. P. Tian, Q. Y. Chen, Q. Zhang, H. Wang, D. Q. Tan, Z. M. Xue, J. Y. Wu, H. P. Zhou, *J. Mater. Chem. C.*, 2015, **3**, 570.
- 31 W. Qin, D. Ding, J. Z. Liu, W. Z. Yuan, Y. Hu, B. Liu, B. Z. Tang, *Adv. Funct. Mater.*, 2012, **22**, 771.
- 32 Y. M. Hong, J. W. Y. Lama, B. Z. Tang, *Chem. Commun.*, 2009, 4332–4353.
- 33 W. Z. Yuan, R. R. Hu, J. W. Y. Lam, N. Xie, C. K. W. Jim, B. Z. Tang, *Chem. Eur. J.*, 2012, **18**, 2847.
- 34 H. Y. Li, Z. G. Chi, B. J. Xu, X. Q. Zhang, X. F. Li, S. W. Liu, Y. Zhang, J. R. Xu, *J. Mater. Chem.*, 2011, **21**, 3760.
- 35 V. Palakollu, S. Kanvah, *New. J. Chem.*, 2014, **38**, 5736.
- 36 S. S. Mati, S. Chall, S. C. Bhattacharya, *Langmuir.*, 2015, **31**, 5025
DOI: 10.1039/C6NJ01558A
- 37 R. R. Hu, N. L. C. Leung, B. Z. Tang, *Chem. Soc. Rev.*, 2014, **43**, 494.
- 38 M. S. Yuan, X. Du, F. Xu, D. E. Wang, W. J. Wang, T. B. Li, *Dyes and Pigments.*, 2015, **123**, 355.
- 39 G. Liu, M. D. Yang, L. K. Wang, J. Y. Wu, Y. P. Tian, *J. Mater. Chem. C.*, 2014, **2**, 2684.
- 40 C. X. Yuan, X. T. Tao, Y. Ren, Y. Li, J. X. Yang, W. T. Yu, *J. Phys. Chem. C.*, 2007, **111**, 12811.
- 41 S. Sasaki, K. Igawa, G. Konishi, *J. Mater. Chem. C.*, 2015, **3**, 5940
- 42 G. Chen, W. B. Li, H. X. Li, W. Z. Yuan, Y. M. Zhang, B. Z. Tang, *Adv. Mater.*, 2015, **27**, 4496.
- 43 J. S. Yang, S. Y. Chiou, and K. L. Liao, *J. Am. Chem. Soc.*, 2001, **124**, 2518.
- 44 J. Chen, C. C. W. Law, J. W. Y. Lam, Y. Dong, S. M. F. Lo, I. D. Williams, D. Zhu and B. Z. Tang, *Chem. Mater.*, 2003, **15**, 1535.
- 45 G. Yu, S. Yin, Y. Liu, J. Chen, X. Xu, X. Sun, D. Ma, X. Zhan, Q. Peng, Z. Shuai, B. Z. Tang, D. Zhu, W. Fang and Y. Luo, *J. Am. Chem. Soc.*, 2005, **127**, 6335.
- 46 F. Xu, H. Wang, X. C. Du, W. J. Wang, D. E. Wang, S. Chen, X. H. N. Li, M. S. Yuan, J. Y. Wang, *Dyes and Pigments.*, 2016, **129**, 121
- 47 Y. Liu, X. T. Tao, F. Z. Wang, X. N. Dang, D. C. Zou, Y. Ren, M. H. Jiang, *J. Phys. Chem. C.*, 2008, **112**, 3975
- 48 W. Huang, F. S. Tang, B. Li, J. H. Su, H. Tian, *J. Mater. Chem. C.*, 2014, **2**, 1141–48.
- 49 X. Zhao, P. C. Xue, K. Wang, P. Chen, P. Zhang, R. Lu, *New. J. Chem.*, 2014, **38**, 1045
- 50 X. Zhang, X. P. Gan, S. Yao, W. Zhu, J. H. Yu, Z. C. Wu, H. P. Zhou, Y. P. T, J. Y. Wu, *RSC. Adv.*, 2016, **6**, 60022
- 51 L. K. Wang, Z. Zheng, Z. Yu, J. Zheng, M. Fang, J. Y. Wu, Y. P. Tian, H. P. Zhou, *J. Mater. Chem. C.*, 2013, **1**, 6952
- 52 Z. H. Cao, C. Xu, L. H. Liang, Z. J. Zhao, B. Chen, Z. J. Chen, H. Chen, G. Qu, D. M. Qi, G. R. Shand, U. Zienere, *Polym. Chem.*, 2015, **6**, 6378
- 53 Y. L. Xu, W. Yang, J. Shao, W. Q. Zhou, W. Zhu, J. Xie, *RSC. Adv.*, 2014, **4**, 15400.
- 54 C. Y. K. Chan, Z. J. Zhao, J. K. Y. Lam, J. Z. Liu, B. Z. Tang, *Adv. Funct. Mater.*, 2012, **22**, 378.
- 55 W. Yang, Z. Q. Cheng, Y. L. Xu, J. Shao, W. Q. Zhou, J. Xie, M. Y. Li, *New. J. Chem.*, 2015, **39**, 7488–94.

Sentence:

Three compounds linked to triphenylamine and single, double triple branched 4-(N,N'-dimethylamine) phenyl groups through an imine π -bridge were synthesized, showing effective AIE effect and good fluorescence imaging.

Image